SLAC-PUB-3055
February 1983
(T/E)

SCALAR BOSON PRODUCTION AND DECAY IN COMPOSITE MODELS*

F. M. RENARD
Stanford Linear Accelerator Center
Stanford University, Stanford, California 94305

ABSTRACT

In composite models where vector bosons ($W^{\pm}, Z$) and scalar boson (H) are made of the same subconstituents and especially in W-dominance models we show that couplings like $HZ\gamma$, $H\gamma\gamma$, Hgg can be rather large. As a consequence the decay pattern and the production rates of scalar bosons in e^+e^-, $\gamma\gamma$ and hadron-hadron collisions can be completely different from the standard Higgs case.

Submitted to Physics Letters B

* Work supported in part by the Department of Energy, contract DE-AC03-76SF00515 and by Centre National de la Recherche Scientifique, France.

Recently several arguments have been given in favor of models which consider weak interactions as a residual effect of quark and lepton compositeness [1]-[7]. Composite $W^{\pm}, Z$ boson exchanges between leptons or quarks are the weak analogue of meson exchanges between hadrons during strong interactions. In addition it has been shown that one can reproduce most of the results of the standard model at low energy if one makes the assumption of single W dominance for electroweak processes [6]-[7]. In this note we want to show that such a picture may strongly depart from the standard model when one considers some processes involving composite scalar (or pseudoscalar) bosons. We show that couplings like $ZH\gamma$, $H\gamma\gamma$, Hgg can be rather large so that the decay pattern and the production rates of these scalar bosons will strongly differ from the standard case.

The W-dominance model [6]-[7] (WDM) is the analogue of the old vector meson dominance model (VDM) for photon-hadron interaction. The W^3 neutral boson (which get mixed [5] with the photon into the Z state) enhances the electromagnetic form factors of leptons and quarks (for $s \simeq M_W^2$) through the $\gamma - W^3$ junction (fig. 1). For on-shell photons the WDM relation:

$$g_{\gamma F} = \left(\frac{e g_{\gamma W}}{M_W^2}\right) g_{WF} \tag{1}$$

applied to the state $F = \ell^+\ell^-$ with $g_{\gamma\ell^+\ell^-} = e$ and $g_{W\ell^+\ell^-} = e/\sin\theta_W$ gives the value of the $\gamma - W^3$ junction:

$$\frac{e g_{\gamma W}}{M_W^2} = \sin\theta_W \simeq \frac{1}{2} \quad . \tag{2}$$

It can then be used for any other final state F when a single W exchange is dominant:

$$g_{\gamma F} = g_{WF} \sin\theta_W \quad . \tag{3}$$

See refs. [6]-[7] for more details, isospin and helicity structures and extension to a series of intermediate bosons. The large value of the $\gamma - W$ junction is interpreted [5]-[8] as a consequence of the small W extension (Λ^{-1}) joined to a small W mass ($M_W \ll \Lambda$) which make W^3 and γ states rather similar. This new picture of electroweak unification have important consequences. The well-known fact that weak interactions have a strength comparable to the electromagnetic ones at high energy ($\sqrt{s} \geq M_W$) is now complemented by the reverse: VDM implies that certain photon couplings which a priori could be very small (for example occurring through high order diagrams in the standard gauge model) now become of the same strength as the W ones. In composite models it is natural to expect several anomalous couplings to occur and to be controlled by the value Λ of the compositeness scale. We already gave [9] examples of Z^o decay modes almost negligible in the standard model but appreciable in composite models. WDM has the additional feature of enhancing the structure functions for $s \simeq M_W^2$. In practice this means that these anomalous photon couplings will now be controlled by an effective scale value Λ_{eff} of the order of M_W instead of Λ.

We assume that scalar (or pseudoscalar) bosons (H) exist with not too high a mass [i.e. $M_H = O(M_W)$]. We assume that H bosons and W bosons are made of the same subconstituents. Charged $H^\pm$ states could obviously be produced through their electric coupling ($\gamma H^+ H^-$) or through $\gamma H^\pm W^\mp$ couplings. In e^+e^- annihilation this may require a rather high energy $\sqrt{s} > 2M_H$ or $M_H + M_W$. In this note we concentrate or neutral H^o states. Scalar states may be identified with the Higgs bosons of the standard model but in the following discussion we do not require such a precise connection. We shall just use the standard Higgs couplings for comparison and illustration. In a composite picture dimensionless couplings between bound states can be expressed in terms of overlap integrals of bound state wave functions. So they are in general expected to be of order one when no special constraint applies. For the couplings of H to two vector states we shall use the gauge invariant forms:

$$f\,(e \cdot e'\; k \cdot k' - e \cdot k'\; e' \cdot k)\quad , \tag{4}$$

$$f\; \epsilon^{\mu\nu\rho\sigma}\; e_\mu\; k_\nu\; e'_\rho\; k'_\sigma \tag{5}$$

respectively in the case of scalar and pseudoscalar H (e^μ, e'^μ, k^μ, k'^μ are polarizations and momenta of the vector states). From the preceding arguments we expect that the couplings of H to two W bosons f_{HWW} will be of order M_W^{-1}. This also agrees with the standard case in which we have the Lagrangian term

$$\frac{1}{2}\; g_{HZZ}\; Z^\mu\; Z_\mu\; H^o \quad \text{with} \quad g_{HZZ} = \frac{e}{\sin\theta_W}\left(\frac{M_Z^2}{M_W}\right) \quad . \tag{6}$$

The H-fermion-antifermion couplings (g_{Hff} or $g_{Hff}\gamma^5$) are expected to be affected by a factor m_f/m_W because of the helicity flip character of this coupling (like the fermion mass term). In the standard model for scalar Higgses we have

$$g_{Hff} = \frac{e}{2\sin\theta_W}\left(\frac{m_f}{m_W}\right) \quad . \tag{7}$$

New properties will now arise for the couplings of composite H^o bosons like $HZ\gamma$, $H\gamma\gamma$, Hgg because photons or gluons directly couple with subconstituents in a point-like way. In the standard model these couplings only occur through high order diagrams (with fermion or $W^\pm$ loops) and are very small [10]. In composite models the $HZ\gamma$ coupling is a simple dipole electric transition (for scalar H) or dipole magnetic one (for pseudoscalar H) which can be computed according to the diagram of fig. 2 in terms of H and Z bound state wave function overlap. Using invariant forms (5) or (6) for $HZ\gamma$ couplings one in general expects to have $f_{HZ\gamma} \simeq e/\Lambda_{eff}$ where Λ_{eff} is an effective subconstituent mass or the inverse of an extension radius. For $M_Z > M_H$ we get the partial width

$$\Gamma_{Z\rightarrow H\gamma} = \frac{k^3}{12\pi} f^2_{HZ\gamma} \tag{8}$$

given in table I for different values of Λ_{eff}. Using WDM (fig. 3) and $f_{HWW} = 1/M_W$ one gets

$$f_{HZ\gamma} = \frac{\sin\theta_W}{M_W} \tag{9}$$

and a width of the order of several tens of MeV (table I). For comparison the standard model [10] given $\Gamma_{Z\rightarrow H\gamma} \leq 1\ keV$.

$H\gamma\gamma$ couplings [again defined by eqs. (5) and (6)] are expected to be of order $f_{H\gamma\gamma} \simeq e^2/\Lambda_{eff}$ according to the process of fig. 4. Table II shows the results for the width $\Gamma_{H\rightarrow\gamma\gamma} = (k^3/8\pi) f^2_{H\gamma\gamma}$ using several values of Λ_{eff} and also the results of WDM. WDM is used in two different ways. Firstly we tried a nonrelativistic formulation giving the partial width in terms of bound state wave functions and derivatives at the origin:

$$\Gamma_{H\rightarrow\gamma\gamma} = \frac{4\alpha^2 Q^4}{M_H^2} \, |\phi(0)\, \sqrt{n_c n_H}\,|^2 \tag{10}$$

$$\Gamma_{H\rightarrow\gamma\gamma} = \frac{144\alpha^2 Q^2}{M_H^4} \, |\phi'(0)\, \sqrt{n_c n_H}\,|^2 \tag{11}$$

in the pseudoscalar and scalar cases expectively; n_c and n_H are numbers of color and hypercolor states of the subconstituents, Q^2 is their mean charge squared. $\phi(0)$ is given by the strength of the $\gamma - W$ junction in fig. 1 according to [8]:

$$\left|\phi(0)\, \sqrt{\frac{n_c n_H}{4\pi}}\right| = \frac{M^{3/2}\, \sin\theta_W}{2eQ} \quad . \tag{12}$$

$\phi'(0)$ can be estimated using scaling and chiral symmetry relations

$$|\phi'(0)| \simeq \frac{M}{2\sqrt{6}} |\phi(0)| \ . \tag{13}$$

This gives:

$$\Gamma_{H\to\gamma\gamma} = \frac{\alpha M_H}{2} \sin^2\theta_W \tag{14}$$

$$\Gamma_{H\to\gamma\gamma} = \frac{3\alpha M_H}{4} \sin^2\theta_W \tag{15}$$

in the pseudoscalar and scalar case respectively. Secondly we used a double WDM relation according to fig. 5 taking again $f_{HWW} = 1/M_W$. This gives

$$f_{H\gamma\gamma} = f_{HWW} \sin^2\theta_W = \frac{\sin^2\theta_W}{M_W} \ , \tag{16}$$

and the widths listed in table II. Strong differences appear between these two calculations. They may be due either to the nonrelativistic approximation or to the single W-dominance approximation. There is qualitatively the same problem when computing by the same methods $\pi^o \to \gamma\gamma$, $\eta \to \gamma\gamma$, $\eta_c \to \gamma\gamma, \ldots$ etc. One solution is the use of an extended meson dominance approach with a series of excited intermediate bosons. In spite of these large uncertainties one gets much larger values than with the standard model which gives [10]:

$$\Gamma_{H\to\gamma\gamma} = \frac{\alpha^2 G}{8\pi^3\sqrt{2}} M_H^3 |I^2| \tag{17}$$

with $|I| \leq 1$; see table II.

If subconstituents are colored the $H \to gg$ decay is again given by the process of fig. 4 gluons replacing photons. Rates are obtained by multiplying eqs. (14)

and (15) by the color factor $2\alpha_s^2/9\alpha^2Q^4$. With $Q = 1/2$, $\alpha_s \simeq 0.1 - 0.15$ one gets

$$\Gamma_{H\to gg} \simeq 5\ GeV\ ,\ 12\ GeV \quad \text{for} \quad M_H = 10\ GeV\ ,\ 50\ GeV\ .$$

Again the standard model gives a much weaker value [11]:

$$\Gamma_{H\to gg} = \frac{\alpha_s^2 GN^2}{36\pi^3\sqrt{2}}\ M_H^3\ . \tag{18}$$

For $N = 6$ quark flavors one gets 6.5 keV, 0.36 MeV for $m_H = 10$ GeV, 50 GeV.

By the same methods we can calculate several other multiboson couplings like $HZ\gamma\gamma$, $HZgg$, $HH\gamma\gamma$, $HHZ\gamma, \ldots$ which get enhanced with respect to the standard case.

In order to estimate the total H^o width and the branching ratios we have to add the fermionic decay modes:

$$\text{for scalar } H^o \quad \Gamma_{H\to f\bar{f}} = \frac{p^3}{\pi M_H^2}\ g_{Hff}^2 \tag{19}$$

$$\text{for pseudoscalar } H^o \quad \Gamma_{H\to f\bar{f}} = \frac{p}{4\pi}\ g_{Hff}^2\ . \tag{20}$$

Using the standard couplings (7) and the first two families of leptons and quarks one gets $\sum_f\ \Gamma_{H\to f\bar{f}} \simeq 50\ keV$ for $M_H = 10\ GeV$. For $M_H = 50\ GeV$ adding the b quark one gets 1.6 MeV. For $M_H = 100\ GeV$ adding the t quark (with a 25 GeV mass) one would get 100 MeV. So it appears that in models with colored subconstituents $H \to gg$ can be dominant and lead to a width of several GeV. In models with uncolored subconstituents $H \to \gamma\gamma$ can dominate with a width in the tens of MeV; for very massive H bosons ($M_H > M_Z$) the modes $H \to Z\gamma$ and $H \to t\bar{t}$ can compete with $H \to \gamma\gamma$.

These large electromagnetic and gluonic couplings give us new important ways for producing H bosons. In e^+e^- collisions the dominant mode becomes $e^+e^- \rightarrow H\gamma$ through γ, Z annihilation (fig. 6). The differential cross-section is given by [12]:

$$\frac{d\sigma}{d\Omega} = \frac{\alpha p^3(1+\cos^2\theta)}{16\pi\, s\sqrt{s}}\left[f^2_{H\gamma\gamma} - \frac{2a^Z_e\, f_{H\gamma\gamma}\, f_{HZ\gamma}\, s(s-M^2_Z)}{|D_Z|^2} + \frac{s^2\, f^2_{HZ\gamma}(|a^Z_e|^2+|b^Z_e|^2)}{|D_Z|^2}\right] \quad (21)$$

a^Z_e, b^Z_e are the standard vector and axial Zee couplings, $D_Z = s - M^2_Z + iM_Z\Gamma_Z$ and $f_{H\gamma\gamma}$, $f_{HZ\gamma}$ are the couplings defined by eq. (5) or (6). At the Z peak we get $\sigma \simeq 1\ nb$ when $M_H < M_Z$. This just corresponds to a branching ratio $B_{Z\rightarrow H\gamma} \simeq 3\%$ which follows from the WDM predictions (9) and the standard total Z width of 3 GeV. Even below the Z peak the cross-section due to e^+e^- annihilation through one photon can be appreciable if M_H is small enough:

$$\sigma = \frac{\alpha p^3}{3s\sqrt{s}}\, f^2_{H\gamma\gamma} \quad (22)$$

Well above the threshold ($\sqrt{s} = M_H$) it can approach one unit of R if one takes the largest couplings predicted by WDM eq. (14) or (15). The $H+\gamma$ final state with one hard monochromatic photon and H decaying into two gluons or two photons should be easy to detect.

In $\gamma\gamma$ collisions the process $\gamma\gamma \rightarrow H^o$ also becomes well observable:

$$\sigma(e^+e^- \rightarrow e^+e^-H) = \frac{4\pi^2}{M^3_H}\, yK_{\gamma\gamma}(\sqrt{s}, y)\, \Gamma_{H\rightarrow\gamma\gamma} \quad (23)$$

with

$$K(\sqrt{s}, y) \simeq \frac{2}{y}\left[\left(1+\frac{y^2}{2}\right)^2 \log\frac{1}{y^2} - \frac{1}{2}(1-y^2)(3+y^2)\right]\left(\frac{\alpha}{\pi}\log\frac{s}{m^2_e}\right)^2 \quad (24)$$

if no tagging restriction applies [12]; $y = M_H/\sqrt{s}$. Taking the largest $\Gamma_{H\to\gamma\gamma}$ values of table II one gets rather large cross-sections:

$$\sigma \simeq 1\ nb \quad \text{for} \quad M_H = 10\ GeV \quad \text{at} \quad \sqrt{s} = 30\ GeV \quad ,$$
$$\sigma \simeq 0.06\ nb \quad \text{for} \quad M_H = 50\ GeV \quad \text{at} \quad \sqrt{s} = 100\ GeV \quad .$$

In the case of colored subconstituents the large $\Gamma_{H\to gg}$ width opens the possibility of a copious H production in hadron-hadron collisions through gluon-gluon fusion (fig. 7). We estimate the production rate with [10]-[16]:

$$\left.\frac{d\sigma}{dy}\right|_{y=0} = \frac{\pi^2}{8M_H^3}\ \Gamma_{H\to gg}\ G\left(\frac{M_H}{\sqrt{s}}\right) \quad . \tag{25}$$

Using the gluon distribution $g(x) = (3/x)(1-x)^5$ inside the nucleon we have $G(M_H/\sqrt{s}) = g[1-(M_H/\sqrt{s})]^{10}$ for nucleon-nucleon collisions. For $\sqrt{s} = 500$ GeV, $M_H = 10$ or 50 GeV, $\Gamma_{H\to gg} = 5$ or 12 GeV one gets $d\sigma/dy|_{y=0} = 20\ \mu b$ or 150 nb. Such a large H production in $h+h \to H+X$ should be well identified by a peak in two gluon jets or two photons invariant masses. $\gamma\gamma$ production at large p_T has already been observed [13] at ISR ($\sqrt{s} = 63$ GeV) with a rate $d^2\sigma/dM_{\gamma\gamma}dy|_{y=0} = (8\pm 4)\times 10^{-35}\ cm^2/GeV$ for $8 \leq M_{\gamma\gamma} \leq 11\ GeV$. This rate (consistent with QCD calculations [14] using $q\bar{q} \to \gamma\gamma$ and other radiative processes) is much smaller than the one we expect from a 10 GeV scalar state with a branching ratio $B_{\gamma\gamma} = \Gamma_{H\to\gamma\gamma}/\Gamma_{H\to gg} \simeq 3\times 10^{-3}$: $d\sigma/dy|_{y=0} \simeq 1.2\times 10^{-32}\ cm^2$. Hence a scalar state with this M_H value and those couplings already seems to be excluded.

Several other models predict the existence of scalar or pseudoscalar mesons with properties notably different from the standard ones, see for example multi-Higgs models [15], technicolor models [16], supersymmetry models [17]. Decay widths and production rates are generally much smaller than the ones here obtained with WDM. So any experimental signal for such anomalous $Z\gamma$, $\gamma\gamma$ or gg processes would be a good indication for this kind of composite models. In such a case precise measurements of $W^{\pm}$ and Z properties especially their multiboson couplings ($ZZ\gamma$, $\gamma^* Z\gamma$, $Z\gamma\gamma\gamma$, $Z\gamma gg$, $Zggg, \ldots$) could confirm the actual picture. In any case it would be interesting to have experimental limits on masses and couplings of such objects.

ACKNOWLEDGEMENTS

We thank Professor S. Drell for hospitality and encouragements, Professor E. Bloom for experimental discussions, Dr. B. Pire for informations about the ISR experiment and colleagues at SLAC Theory Group for comments and discussions.

REFERENCES

1. *General reviews*: M. E. Peskin, Proceedings of the 1981 International Symposium on Lepton Photon Interactions, Bonn, ed. by W. Pfeil (1981); L. Lyons, Oxford University 52/82 (1982).
2. H. Fritzsch and G. Mandelbaum, Phys. Lett. 102B (1981) 319; H. Fritzsch, R. Kögerler and D. Schildknecht, Phys. Lett. 114B (1982) 157.
3. L. Abbott and E. Farhi, Phys. Lett. 101B (1981) 69.
4. R. Barbieri, R. N. Mohapatra and A. Masiero, Phys. Lett. 105B (1981) 369.

5. P. Q. Hung and J. J. Sakurai, Nucl. Phys. B143 (1978) 81; P. Chen and J. J. Sakurai, Phys. Lett. 110B (1982) 481; J. J. Sakurai, MPI-PAE-PTh 22/82 (1982).

6. R. Kögerler and D. Schildknecht, CERN-TH-3231 (1982).

7. M. Kuroda and D. Schildknecht, Phys. Lett. 121B (1983) 173.

8. H. Fritzsch, CERN-TH-3219; talk given at the 2nd Europhysics Study Conference on Unfication of Fundamental Interactions, Erice (1981).

9. F. M. Renard, Phys. Lett. 116B (1982) 269; Nucl. Phys. B196 (1982) 93.

10. G. Barbiellini et al., ECFA/LEP Report, DESY 79/27 (1979).

11. F. Wilczek, Phys. Rev. Lett. 39 (1977) 1304.

12. F. M. Renard, Basics of e^+e^- Collisions, ed. by Frontieres (1981).

13. C. Kourkoumelis et al., CERN EP/82-108 (1982).

14. A. P. Contogouris, L. Marleau and B. Pire, Phys. Rev. D25 (1982) 2459.

15. J. A. Grifols and R. Pascual, Z. Phys. C6 (1980) 353.

16. G. Barbiellini et al., ECFA/LEP Report, DESY 81-064 (1981).

17. Proceedings of the CERN Workshop on Supersymmetry, CERN-TH-3311/EP 82/63 (1982).

TABLE I

$\Gamma_{Z \to H\gamma}$ Decay Widths

	Λ_{eff} = 1 TeV	$\Lambda_{eff} = M_W$	WDM	Standard Model
m_H = 10 GeV	0.22 MeV	35 MeV	87 MeV	≤ 1 keV
m_H = 50 GeV	0.07 MeV	11 MeV	28 MeV	

TABLE II

$\Gamma_{H\to\gamma\gamma}$ Decay Widths

	$\Lambda_{eff} = 1$ TeV	$\Lambda_{eff} = M_W$	WDM[(1)]	WDM[(2)]	Standard Model
$m_H = 10$ GeV	0.04 keV	6.3 keV	14 MeV	39 keV	≤ 2 eV
$m_H = 50$ GeV	.5 keV	0.8 MeV	70 MeV	4.9 MeV	≤ 0.2 keV

(1) From eq. (15).

(2) From eq. (16).

FIGURE CAPTIONS

1. $W^3 - \gamma$ junction in composite models.
2. Radiative transition $Z \to H\gamma$ in composite models.
3. Radiative transition $Z \to H\gamma$ in W-dominance models.
4. $H \to \gamma\gamma$ decay process in composite models.
5. $H \to \gamma\gamma$ decay process in W-dominance models.
6. Diagram for $e^+e^- \to H\gamma$.
7. H production in hadron-hadron collisions through gluon-gluon fusion.

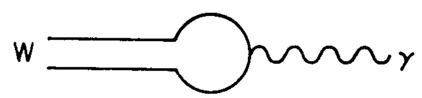

Fig. 1

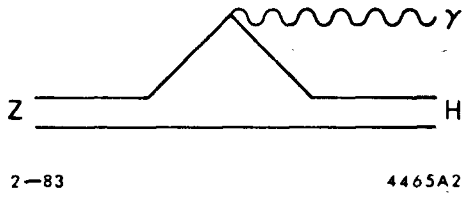

Fig. 2

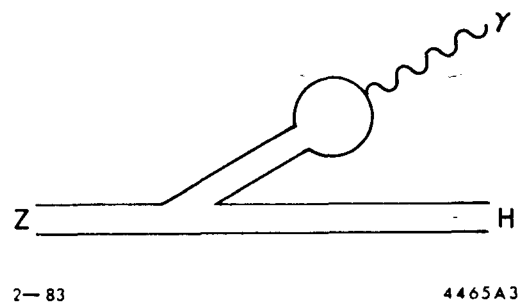

Fig. 3

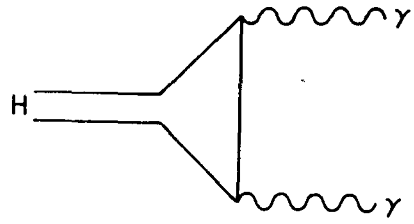

Fig. 4

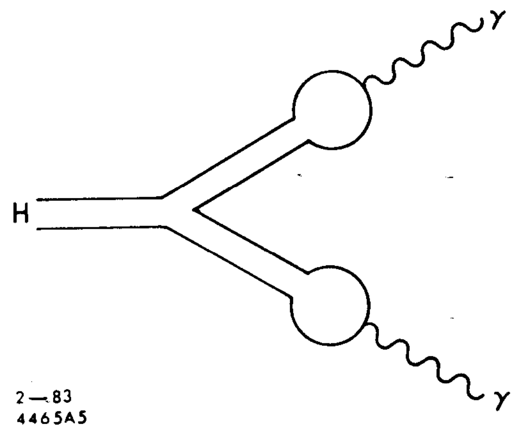

Fig. 5

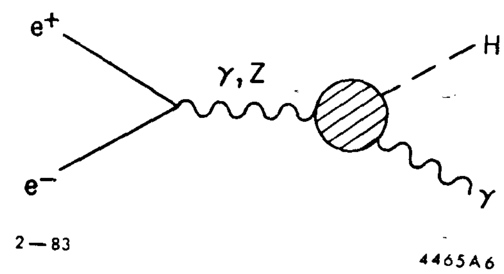

Fig. 6

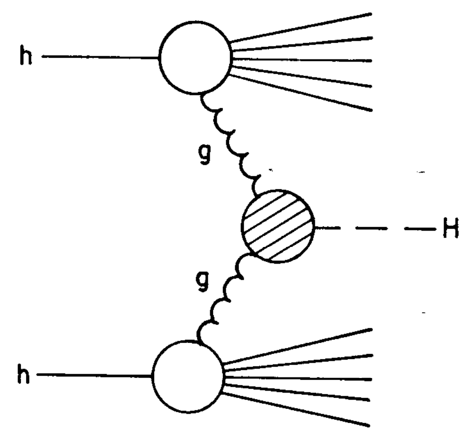

Fig. 7